ACTA IMEKO
ISSN: 2221-870X
March 2025, Volume 14, Number 1, 1 - 17

Spectral emissivity measurement for high-temperature applications: a systematic review

N. Giulietti[1], G. Cosoli[2,3], R. Napolitano[3], G. Pandarese[3], G. M. Revel[3], P. Chiariotti[4]

[1] *Dipartimento di Ingegneria Industriale e dell'Informazione, University of Pavia, 27100, Pavia, Italy*
[2] *Department of Theoretical and Applied Sciences, eCampus University, Novedrate, Italy*
[3] *Department of Industrial Engineering and Mathematical Sciences, Università Politecnica delle Marche, 60131 Ancona, Italy*
[4] *Department of Mechanical Engineering, Politecnico di Milano, 20156 Milan, Italy*

ABSTRACT
Measuring emissivity is pivotal for obtaining reliable high-temperature measurements through non-contact techniques such as pyrometry and thermal imaging. The interest in characterizing materials in terms of their radiant properties has increased in recent years due to the expanded application fields of these techniques, ranging from the process industry to aerospace and the energy industry. Various methods are available in the literature to assess material emissivity, but they are primarily classified into indirect and direct methods. This review also addresses different types of materials, various experimental conditions (e.g., heating technologies and measurement frequency bands), and different types of measurement outputs. The aim of this review paper is therefore to systematically examine the literature available on the topic, highlighting the pros and cons of the different methodologies used for measuring emissivity at temperatures up to 2500 °C.

Section: RESEARCH PAPER

Keywords: Spectral emissivity measurement; high temperature measurement; measurement uncertainty

Citation: N. Giulietti, G. Cosoli, R. Napolitano, G. Pandarese, G. M. Revel, P. Chiariotti, Spectral emissivity measurement for high-temperature applications: a systematic review, Acta IMEKO, vol. 14 (2025) no. 1, pp. 1-17. DOI: 10.21014/actaimeko.v14i1.1846

Section Editor: Antonio Cannuli, Università degli Studi di Messina, Italy

Received March 22, 2024; **In final form** May 22, 2024; **Published** March 2025

Funding: This research activity was carried out within the DESTINY (Development of an Efficient Microwave System for Material Transformation in energy INtensive processes for an improved Yield) project, funded by the European Union's Horizon 2020 research and innovation programme under grant agreement no 820783.

Corresponding author: Paolo Chiariotti, e-mail: paolo.chiariotti@polimi.it

1. INTRODUCTION

An accurate understanding of the radiation properties of a material, such as its emissivity, plays a pivotal role in many industrial and engineering applications targeting quantitative temperature measurements and the assessment of radiated heat transfer. In fact, each object emits thermal electromagnetic radiation differently, and the assessment of its optical properties is essential for obtaining the actual surface temperature. Depending on the working temperature and surface roughness (which determine the surface optical response to given wavelengths), some methods may be more suitable than others [1], emphasizing the importance of knowing the emissivity to achieve accurate high-temperature radiation sources for calibrating radiation-based thermometers. Particular attention has been paid to silicon photodiodes (usable in the range of 300-1100 nm). Fixed-point radiators can be used to maintain constant radiation, thus supporting the realization of accurate radiance and irradiance scales [2]. On the one hand, contact sensors, such as thermocouples (or thermopiles), resistor temperature detector sensors, etc., are widely used as references to obtain accurate surface temperature measurements [3]-[6]. On the other hand, their application is limited to temperatures up to 1500 °C, as in high temperature applications both convective heat losses and performance degrade due to possible corrosion phenomena, resulting in higher measurement uncertainty. For this reason, the scientific community has invested significant effort in recent years to try to exploit non-contact infrared methods. However, this requires improving the reliability of radiant emissivity data [7]. Industrial furnaces represent an application where the characterization of material radiant properties is particularly relevant. Indeed, the use of high-emitting surfaces reduces fuel consumption and heating times, thus increasing the performance

and efficiency of furnaces [8]. Conversely, low-emitting materials are widespread for obtaining high-temperature solar absorbers in solar plants [9]. Another important application where an accurate knowledge of material emissivity is of key importance targets the protection of critical components against overheating, such as alloy-based constituents used in various technological systems of the aerospace industry [10], [11]. High working temperatures significantly affect the material radiant behaviour. However, other factors strongly influence actual emissivity, such as spectral range, emission angle, surface composition, and the geometry of the target. There is considerable interest in high-temperature applications within the industry, as evidenced by numerous studies and projects in this field. For example, the HiTeMS (High Temperature Measurement Solutions for Industry) project aimed at developing techniques to enhance industrial thermometry up to 2500 °C [12]. The InK2 (Implementing the new Kelvin 2) project considered aspects related to measurement uncertainty in high-temperature industry (430-1358 K) by employing radiometric primary thermometry methods [13]. Assessing radiant emissivity and correctly utilizing it in a measurement chain involving non-contact systems is not an easy task. This paper discusses the main studies dealing with this topic with the aim to assist users in properly performing non-contact temperature measurements by focusing on the primary strategies for accurately measuring emissivity. The paper is organized as follows: Subsections 1.2 and 1.3 provide a general description of the physics behind radiant emissions and an overview of the radiant behaviour of different materials. Sections 2 and 3 summarize the main emissivity measurement approaches, classified into two main clusters: indirect and direct methods. The primary measurement systems discussed in the literature are reported, focusing on the characteristics of the tested materials (phase, smoothness, roughness, transparency, presence of oxide film or coatings) or on the type of measured emissivity (directional, hemispherical, spectral, and total emissivity). The differences in terms of adopted heating technology and measurement conditions (temperature and wavelength ranges) are also highlighted. Finally, Section 4 summarizes the advantages and drawbacks of the different methodologies, focusing on their measurement accuracy.

The radiation emitted by a material depends on its surface treatments and temperature [14]. An ideal emitter and absorber for each temperature and wavelength, regardless of direction, is generally defined as blackbody. This peculiar characteristic makes blackbodies highly useful as reference targets. The spectral emissive power of a blackbody is described by the Planck's law (Equation 1).

$$W_0(\lambda) = \frac{2\,\pi\,h\,c^2}{\lambda^5(\mathrm{e}^{h\,c/(\lambda\,k\,T)} - 1)}, \text{in W m}^{-2}\,\mu\text{m}^{-1}\,, \tag{1}$$

where h = 6.6 × 10^{-34} J s is the Planck constant, c = 3 × 10^{8} m s^{-1} is the speed of light in the vacuum, k = 1.4 × 10^{-23} J K^{-1} is the Boltzmann constant and T is the absolute temperature. The maximum emittance shifts towards shorter wavelengths as the temperature increases, extending up to the visible range. This can be demonstrated by differentiating the Planck's law equation with respect to λ and obtaining the Wien's law, which is related to the maximum radiation intensity for a given temperature:

$$\lambda_{\max}\,T = cost = 2897.6\ \mu\text{m K}. \tag{2}$$

The Stefan-Boltzmann law is obtained by integrating the Planck's law over the entire wavelength range. It describes the total emittance of a blackbody as a function of temperature:

$$W_0(T) = \int_0^\infty W_0(\lambda, T)\,\mathrm{d}\lambda = \varepsilon\,\sigma\,T^4 = \sigma\,T^4\,, \tag{3}$$

where ε is the maximum emissivity value, equal to 1, σ = 5.7 × 10^{-8} W m^{-2} K^{-4} is the Boltzmann constant and T is the absolute temperature expressed in *K*.

When considering a real body, the energy emitted is always less than that emitted by a blackbody at the same temperature, as a portion of the energy is partially reflected, while another fraction can be transmitted and absorbed. The energy balance of the incident radiation of a real body can be expressed as the sum of the three contributions:

$$\alpha + \gamma + \tau = 1\,, \tag{4}$$

where α, γ and τ are the absorbed, reflected, and transmitted amounts of energy, respectively. The three coefficients depend on the nature of the body, its temperature, and the wavelength of the radiation. Therefore, it is possible to define materials with $\tau = 0$ as opaque (or grey bodies), while those with $\tau = 1$ are transparent. On the other hand, semi-transparent materials act as selective radiators, depending on different wavelength regions.

Considering an opaque material, Kirchhoff's law states that the absorbed energy is equal to the emitted energy at thermal equilibrium, so that $\alpha = \varepsilon$. In this case, the Stefan-Boltzmann law for an opaque material (or grey body) becomes as reported in Equation 5.

$$W(T) = \int_0^\infty W(\lambda, T)\,\mathrm{d}\lambda = \alpha\,\sigma\,T^4 = \varepsilon\,\sigma\,T^4\,, \text{in W m}^{-2}. \tag{5}$$

When considering both the spatial and spectral domains, it is possible to define the total hemispherical emissivity as the ratio of the power emitted by the material to that emitted by the blackbody in all directions and for all wavelengths, as a function of temperature (Equation 6)

$$\varepsilon(T) = \frac{W(T)}{W_0(T)}\,. \tag{6}$$

The total hemispherical emissivity can be approximated to the total normal emissivity for a perfectly smooth (specular) surface that depends only on the normally incident radiation. For a given wavelength, it is possible to define the hemispherical monochromatic emissivity, expressed as a function of temperature and wavelength. The fraction of the total emissive radiation within a wavelength range ($\lambda_1 < \lambda < \lambda_2$) is called spectral emissivity.

When considering non-isotropic and polarized surfaces, it is necessary to express the energy emitted in a given angular direction and wavelength, defining the directional spectral emissivity as a function of the zenith angle θ and azimuthal angle ϕ. Generally, a blackbody is a perfect diffuse emitter, so its radiation intensity does not depend on the incidence direction. Similarly, the total directional emissivity can be expressed as the ratio of the power radiated by the material and the blackbody, at a given temperature and incidence direction.

Given that the focus of this review paper is on high-temperature applications, it is important to provide an overview of the emissive behaviour concerning temperature and wavelength of the various materials tested in literature in this area. Some experimental data on the radiant behaviour of different materials at high temperatures are reported in [15]. The industry interest in characterizing the thermophysical properties of materials up to high temperatures (approximately 3000 °C) is

demonstrated by research projects like Hi-TRACE (https://hi-trace.eu/), where emissivity of materials is investigated, along with thermal diffusivity and thermal contact resistance [16]. In general, two types of reference materials are used for their known emissivity:

- high-emissivity materials, designed to provide high stability in thermal processes, can be used as blackbody radiators if applied to the inner walls of a cavity [8] or exploited on metal surfaces to improve the accuracy of temperature measurements [17];
- low-emissivity materials with high reflectivity are mainly used when a reduction in infrared radiation is required [18].

Generally, these materials are used in high-temperature applications as coatings. These coatings are composed of non-conductive materials (ceramic, inorganic composites, etc.), while various pure metals and alloys are used in the constituents of low-emissivity coatings. Many researchers have investigated the performance of these reference materials to verify their durability at high temperatures and highlight any eventual degradation.

In general, the emissivity of these coatings does not change over the spectral range, although in some works, a different behaviour has been demonstrated. [19]-[22]. However, higher emissivity variations are shown in the wavelength region higher than 20 μm. The main factors that affect the optical properties of these materials are oxidation phenomena, which occur at high temperatures, or surface roughness [9], [11], [23]-[29], since the higher the oxidation and roughness, the higher the emissivity. However, their surface conditions at high temperatures influence the spectral emissivity more than the absolute total emissivity. Peng et al. [25] demonstrated that the infrared emissivity of coatings made from carbonyl iron powders decreases with increasing annealing temperature. The thickness of these films (applied on different substrates) influences the heat-resistance properties [30]-[32]. The lower influence of metal substrates with increasing coating thickness of high-emissivity layers was demonstrated in [33] and [34].

On the other hand, metallic surfaces exhibit a different behaviour. In general, several studies have shown that the expected emissivity trend of conductive layers on a semi-transparent substrate monotonically decreases with increasing wavelength, while it increases with increasing temperature [35]-[41].

However, variations in the elements, concentration, and layer composition result in different types and degrees of oxidation and varying magnitudes of spectral emissivity. Furthermore, surface finish, purity of the investigated samples, and their state evolution are other important factors that must be considered: spectral variations are far less pronounced for extruded and saw-cut surfaces, while emissivity is generally lower for polished samples and increases with increasing roughness. Brodu et al. demonstrated that increasing surface roughness (starting from a flat surface) progressively gives more weight to longer wavelength range emissivities (> 2.8 μm) than to shorter wavelength ones (< 2.8 μm) [28].

The methodologies adopted for measuring emissivity are discussed in the following sections. These methods are clustered into indirect and direct methods according to the physical principle of the measurement approach used. A diagram illustrating the different methods adopted for characterizing emissivity is shown in Figure 1.

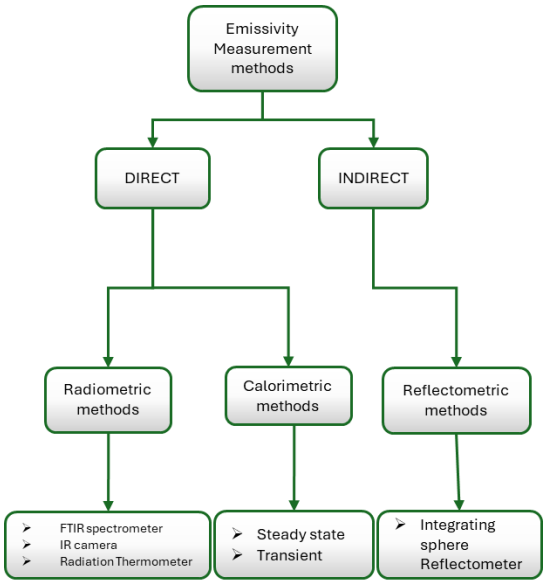

Figure 1. Scheme of the main methods used for emissivity characterisation.

2. INDIRECT METHODS

Indirect methods exploit the most common technique for determining emissivity from reflectivity and transmissivity by using the Kirchhoff's law. The directional hemispherical reflectivity is most commonly used for the indirect experimental determination of emissivity with respect to directional spectral absorption, primarily because it shares the same mechanism of interference with external source radiation as absorptivity [42].

The indirect emissivity measurements are generally performed with an external input beam source that illuminates the sample inside an integrating sphere system, which measures the directional hemispherical reflection (Figure 2). The sample is uniformly illuminated with an incidence angle of 8-12° (close to 0°) with respect to the normal; a detector on the side of the spherical cavity measures all the sample multiple reflections in the Ultraviolet/Visible/Near Infrared (UV-VIS-NIR) spectral range. A baffle, generally located between the input and the detector ports, shields the detector from direct radiation.

Considering a real sphere, different sources of error may influence the measurement accuracy, depending on the type of diffuse reflective coating selected to cover its internal cavity, as well as on the non-ideal geometry, including the design of the non-reflecting ports [44]. For this reason, various works have aimed at investigating the system design, methods, and limitations of integrating sphere instrumentation, examining its throughput depending on the application field. Table 1 lists the main data of the different indirect measurement systems and the adopted parameters, along with the related references.

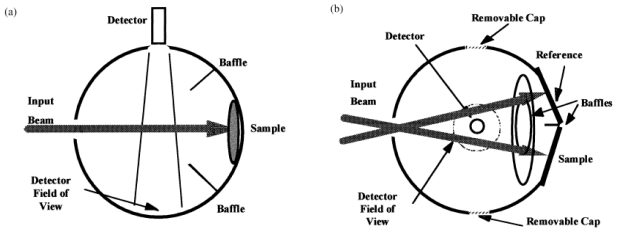

Figure 2. Example of integrating sphere configuration: side (a) and top (b) views [43].

Table 1. Summary of indirect emissivity measurement systems.

Reference	Measurement methods and devices	Temperature range (°C)	Spectral range (μm)	Investigated materials	Measurement uncertainty
	-		4-14	Black paint (Nextel Velvet Coating 811-21)	
[45]	- FTIR spectrometer (Bomem DA3) - Sphere reflectometer - Diode laser source - Filter radiometers - BB sources - Gas purge lines	327-1127	1-20	Opaque samples	2.5 %
[46]	- Sphere reflectometer - Filter radiometers - Halogen lamp source - Reference sample (specular gold mirror)	150-1000	0.90-1.55	Pt–10 %Rh	0.72 % (at 600°, *k* = 2)
				SiC	0.70 % (at 600°, *k* = 2)
[47]	- FTIR spectrometer (Bomem DA3) - Sphere reflectometer - Filter radiometers - BB sources	300-900	2-20	Pt–10 %Rh	± 2.92 %
				SiC	± 0.93 %
[48]	- Optical system - Reflector used as dummy light source - thermocouples	427-927	1.5	Polished aluminium sheet, roughened steel and polished steel	-
[49]	- Tungsten halogen lamp - Monochromator - Integrating sphere with cooling systems - Sample furnace - Control system	27-627	0.4-10	Solar absorbing coatings	5.3 % (*k* = 2)
[50]	- Spectrophotometer Lambda950 (Perkin Elmer) - Integrating with cooling systems - Temperature controller - Heater sample holder	up to 500	0.3-2.5	Two metallic absorbers with selective coatings Refractory materials (SiC and α-Al_2O_3) Metallic: oxidized stainless steel	-

Despite the plethora of scientific articles dealing with the assessment of emissivity at ambient temperature [19], [43], [51]-[55], this is not the case for high-temperature applications, which is the main topic of this paper. Nevertheless, some recent works exploit indirect emissivity characterization as a supplement to the direct radiometric method. In [45], [46], the integrating sphere reflectometer developed at NIST was equipped with a radiometric facility for temperature-dependent emittance measurements of opaque, specular, and diffuse samples, up to 1000 °C. A higher measurement accuracy was obtained compared to that measured by a thermocouple installed inside the sample. The first results were achieved for SiC and Pt–10 %Rh, which are both generally adopted as emittance standard reference materials for high temperatures [47]. A different experimental apparatus, exploiting a reflector as a dummy light source and a detector as an optical detection system, was proposed by Shi et al. [48]. The apparatus included heating, temperature-controlling, and angle-adjusting systems to warm up the tested opaque materials over the 427-927 °C temperature range at a given wavelength of 1.5 μm. A similar system was built at the Harbin Institute of Technology (HIT) to measure the spectral emissivity of high solar absorber coatings from ambient temperature up to 627 °C [49]. The main difference was the choice of temperature and spectral ranges, carefully selected for solar absorber materials. In [50], a specific heating sample holder was adopted on the integrating sphere spectrometer for heating the solar absorber samples at temperatures up to 500 °C. To avoid the degradation of the sphere internal surface, covered by Spectralon® (a diffuse reflectance material very sensitive to high temperatures), the sample holder was placed on the top of the sphere only for a few minutes during the spectral acquisition, and a water-cooling system was foreseen.

3. DIRECT METHODS

Direct radiometric methods encompass a wide variety of techniques involving diverse sample types and spectral and temperature ranges of interest. The methods differ in multiple aspects, such as the practical realization of sample heating, the eventual use of the blackbody, the sample surrounding, and the instrumentation required to achieve spectral and, if applicable, angular and lateral resolution. When used, the blackbody is typically stabilized at the same temperature as the sample; moreover, the sample and the blackbody can be compared at different temperatures to achieve approximately equal total radiation levels.

3.1. Calorimetric methods

The calorimetric method provides the entire radiative exchange of a sample surface to reach thermal balance without using any reference blackbody. These techniques are limited to the measurement of the total hemispherical emissivity, being sensitive neither to the angular dependence nor to spectral thermal properties. According to the heat transfer conditions of the sample, they can be divided into steady-state and transient techniques. In the former, the total hemispherical emittance is obtained by measuring the radiant heat flux from the sample to the environment at a given steady-state temperature, whereas in the latter, the specimen is heated to the desired temperature and

Table 2. Summary of calorimetric methods for total hemispherical emissivity measurement.

Reference	Measurement methods and devices	Temperature range (°C)	Investigated materials	Experimental error
[56]	- Heat-flux sensor - Minco Products' flexible heaters - Vacuum chamber - Dewar flask	-50- 60	Black paint and Electrostatic Switched Radiator (ESR) device	-
[57]	- Steady-state calorimetry - Sheet heater	-100-427	Thin polyimide film coated with aluminium on the back surface	5.0 % and +3.5 % (overall uncertainty)
[58]	- Steady-state calorimetry - Mica heater	77-377	Aluminium alloy (Anticorodal 6063)	8-12 % (for ε ≈ 0.05) 4-5 % (for ε ≈ 0.1) 2-3 % (for ε > 0.3)
[59], [60]	- Steady-state calorimetry - AC power source with electric current for heating	427-1027	Conductive materials (nickel and steel) as thin strips	1.1 %
		297- 1057	Iron-based alloy (21 % chromium, 6 % aluminium) samples	< 1.6 % (decreasing with increasing temperature)
		427-1027	Nickel samples	0.04-0.13 % from simulation 0.17-2.36 % with random noise 0.02-0.22 % in experiments 1.03-1.08 % analytical uncertainties
[61]	- Steady-state calorimetry - DC power source with electric current for heating	above 1000	Type 304 stainless steel and molybdenum	-
[1]	- Steady-state calorimetry - Heat sink	35-75	Thermal insulating coating	-
[62]-[64]	- Combined transient and steady-state calorimetry - feedback control system - DC power source and current switch - pyrometer - laser ellipsometer	1727-2527	Tantalum specimen	± 5 %
		1527-2527	Strip-shaped specimens of tantalum and molybdenum	± 2 % for tantalum ± 4 % for molybdenum
		1227	Molybdenum	± 5 %
[31]	- Steady-state calorimetry - Vacuum chamber - Kramers-Kronig analysis and virtual mode equations	127-477	Vycor glass	< 1 %
			Fused silica glass	< 1.5 % at 127 °C ≈ 7 % at 477 °C
[65]	- Steady-state calorimetry - Thermal guard rings with wire guard block	-20-200	opaque solid materials	Expanded uncertainty between ± 0.005 and ± 0.03
[66]	- Steady-state calorimetry - Thermal guard rings with wire guard block - Reflectometric techniques	Room temperature	Polished aluminium PVC Sand blasted aluminium Aluminium paint	0.025 (for aluminium samples) 0.08 (for PVC)
[67]	- Steady-state calorimetry - Electrical heaters - Outer cylindrical stainless-steel tube	up to 450°C	Coated solar thermal cylindrical absorber samples	± 13 % (k=2)
[32]	- Transient calorimetry - Modified furnace	57-497	Glass sheets (borosilicate)	up to 2.9 %
[68]	- Transient calorimetry - AC power source	177-677	Ferromagnetic materials samples, in particular a steel strip	< ± 9.4 %,
[69]	- Combined transient and steady-state calorimetry - Mica heater	27-427	Aluminium alloy (Anticorodal 6063) and Inconel 718	8-12 % (for ε ≈ 0.05) 4-6 % (for ε ≈ 0.1) 2-3 % (for ε > 0.3)
[70]	- Transient calorimetry - Numerically computed transient response	47-157	Polished aluminium, aluminium paint, and blackboard paint	0.03 (polished aluminium) 0.02 (aluminium paint) 0.04 (blackboard paint)

subsequently cooled, hence obtaining the heat flux density from the temperature decay measurement (this is particularly suitable for metallic specimens as a very small thermal gradient occurs). The different calorimetric methods are summarized in Table 2.

3.1.1. Steady-state techniques

Different experimental apparatuses for steady-state measurements have been developed over the years. Generally, the tested samples are suspended at mid-height of a test chamber cooled by a liquid nitrogen cryostat, kept under vacuum, and with inner walls painted black [57], [58]. One or more thermocouples are attached to the sample and to the inner wall in order to check the uniform temperature distribution generated by the heating system. In [68], the temperatures acquired by the inner thermocouples were calibrated using an outer cylindrical stainless-steel tube with three thermocouples soldered in front of the tube wall in the same positions as the inner ones and wrapped with insulation. An expanded uncertainty (coverage factor $k = 2$)

of ± 13 % was obtained for the total hemispherical emittance at a temperature of 300 °C. At low temperatures, Moghaddam et al. proposed an alternative to directly measure the emissivity of the thermal isolation of the structure [56]; in particular, they used a heat-flux sensor passing through active (ESR device) and passive (black paint) surfaces. As the temperature uniformity of the sample is fundamental to obtain accurate emissivity results (particularly when operating at high temperatures), different works suggest selecting the sample centre as the investigated region, avoiding errors due to the non-uniform temperature distribution[59], [61], [71], [72]. When the steady-state techniques are applied to metal samples with a thin protective layer, it is necessary to consider the evaporation of the layer at high temperatures. Otsuka et al. [61] investigated the hot-filament method for heating samples in a shorter heating time. They proposed to use a current that directly passes through the sample and two copper electrodes (two sets of thermocouples) for deleting the influence of the heat loss caused by the water-cooled electrode. On the other hand, Matsumoto et al. [62]-[64] proposed a combined transient and quasi-steady-state method to achieve very high temperatures (up to 2500 °C) in a very short time (< 1 s) using a feedback-controlled pulse-heating system. In [64], the conductive heat loss in the brief steady-state, which causes an error in emissivity measurement, was also analysed. In [31], the thermal conductivity of a disk-shaped sample (Vycor and fused silica glass surfaces) was derived from the hemispherical total emissivity. The bottom face of the sample was blackened and coated with a metallic material (copper) to ensure conductive heating. Fu et al [60] proposed a method to simultaneously measure the total hemispherical emissivity and thermal conductivities of conductive samples at high temperatures; if thermal conductivity is known, emissivity and temperature distribution can be determined from the inverse solution of the energy equation; otherwise, both thermal conductivity and emissivity can be expressed as functions of temperature. The main innovation was the adoption of two thermal guard rings surrounding the two samples and reducing the thermal perturbations for a more accurate measurement of the mean surface temperature. A model with related uncertainty of 0.11 % was used for the estimation of total hemispherical emissivity.

In [66] this apparatus was used on four types of materials, and the results were compared with those indirectly obtained through reflectometric techniques. A relatively large uncertainty (0.08) was observed for the spectral emissivity of conductive materials (i.e., low-emissive and very specular, such as aluminium paint). Monchau et al. [67] compared the total hemispherical emissivity results obtained by calorimetric, absolute/relative reflectometric, and directional reflectometric measurement methods, highlighting that the results were affected by non-negligible uncertainties and were also quite scattered. However, they noted that the spectral reflectometric technique is faster and easier to use compared to calorimetry.

3.1.2. Transient techniques

As mentioned above, transient calorimetric techniques are generally adopted for the emissivity measurement of metallic materials, as surface temperature is nearly uniform during the cooling process, contrary to non-conducting materials. On the other hand, Masuda et al. [32] demonstrated how an improved version of this technique can be used for non-conducting materials (e.g., glass sheets) by considering only the beginning of the specimen cooling for emissivity evaluation due to the lower temperature gradient; the related error was estimated to be up to 2.9%. In [69], ferromagnetic material samples were tested using known values of specific heat at different temperatures taken from the literature. However, the steady-state method is more accurate than the transient one above the Curie temperature, at which the ferromagnetic material loses its ferromagnetism and becomes paramagnetic [73]. Tanda and Misale [64] adopted the combined transient and steady-state techniques to determine the specific heat of the specimens from the time history of the sample temperature during cooling. Finally, Venugopal et al. [74] utilized the Levenberg–Marquardt iterative procedure to retrieve the heat loss parameters and the total hemispherical emissivity, thereby comparing numerical and experimental results as a function of temperature.

3.2. Radiometric methods

The radiometric methods are the most commonly used for characterizing emissivity at high temperatures across a wide spectral range. They involve the direct comparison of radiation from the investigated sample with that from a reference blackbody, typically stabilized at the same temperature. Several relevant factors should be considered when distinguishing among the main approaches used for radiometric techniques.

The first factor pertains to the practical realization of the blackbody source, which generally involves a small aperture in a graphite block embedded in a SiC cavity (i.e., the furnace) or an ideal radiation absorber painted on a flat plate. As mentioned above, the use of high-emissivity coatings is widespread as a reference and constitutes an important tool to ensure the reliability of radiometric techniques. However, when considering a painted target surface, its ideal radiant properties may be negatively affected by a non-uniform temperature distribution. Therefore, the design of the sample heating and temperature control is also crucial. The heating system can be implemented with or without a confined space, using, for example, a furnace or a laser heating source, respectively [73]. Generally, thermocouples and temperature controllers can be adopted to monitor and ensure the desired heating of the system, while a water-cooling system is employed in the optics chamber to minimize background radiation and prevent the overheating of the optical components.

Radiometric methods can be categorized based on the different acquisition devices utilized for measuring emissivity, such as FTIR spectrometers, infrared cameras, or pyrometers, which are selected according to the spectral range, target temperatures, and the sample material under investigation.

3.2.1. FTIR spectrometer

Fourier-transform infrared (FTIR) spectroscopy is widely used for the direct assessment of the infrared emission spectrum of both opaque and semi-transparent samples in the NIR and MIR regions. Various strategies have been developed to optimize spectroscopic systems, ensuring accurate system responses and minimizing the main issues linked to sample temperature homogeneity, background radiation, and temperature differences between the sample and blackbody radiator. Moreover, the issues often encountered when using spectrometer instrumentation in material and chemical species characterization are also discussed. Table 3 summarizes the different radiometric methods adopting FTIR spectroscopy reviewed in this article. Since 1990, various studies have evaluated different strategies and heating systems for spectroscopy to minimize errors in emissivity measurements.

Table 3. Summary of direct emissivity measurement systems by using the FTIR spectroscopy (part 1)

Reference	Measurement methods and devices	Temperature range (°C)	Spectral range (μm)	Materials	Experimental error
[75]	- FTIR spectrometer (Thermo Scientific Nicolet iS50) - BB (Isotech R970) - Electric ceramic heater	up to 1127	1.28-28.6	SiC wafer (reference)	Total uncertainty of 1 %
[76]	- Heated sample holder - BB (MIKRON M360) - FTIR with different detectors	21, 327, 527	2-25	SiC wafer (reference) Fabry–Perot resonator	Overall uncertainty: 3 %
[77]	- FTIR spectrometer - BB (RT1500) - Heating furnace - Temp. control system - IR light source - PSAD algorithm (direct method) - SPSO algorithm (inverse method)	450	3-12	Sapphire	--
[78]	- Fiber-Optic spectrometer (DWARF Star NIR) - Blackbody (HF-200C) - Self-designed silicon carbide heater	550-800	0.95-1.6	Wafer, silicon carbide, molybdenum, and tungsten	3 %
[79]	- Fiber-Optic spectrometer (AvaSpec-ULS2048) - Two-colour method	1287, 1307, 1327, 1347, 1377	0.2–1.1	Gasoline flame Coal-burning flame Red phosphorus flame	-
[80]	- Fiber-optic spectrometer (AvaSpec-ULS2048-USB2) - High-speed camera (Edgertronic SX1) - Mikron model M330 blackbody furnace - Bunsen burner	1209-1257	0.5-1	R-type thermocouple	Quasi-steady state heating: 0.32 % (spectrometer) and 0.62 % (camera) Unsteady state heating: 0.55 % (spectrometer) and 0.75 % (camera)
[81]	- Fiber-optic spectrometer (AvaSpec-Mini2048CL) - Mikron model M330 blackbody furnace	1130-1330	0.4-0.9	Three different biomass volatile flames	1.8 %
[82]	- Vacuum emissometer (with BOMEM DA3.02 spectrometer) - CO_2 laser heating - Two-colour pyrometry technique	527-1727	2-20	Oxides: sapphire, spinel, yttria, aluminium oxynitride, fused silica	-
[83]	- CO_2 laser heating - Vacuum chamber - FTIR spectrometer (BRUKER IFS 113V) - BB furnace (Pyrox PY 5)	327-2727	0.83-1000	Silica (SiO_2) Alumina (Al_2O_3) Magnesia (MgO)	-
[84]	- FTIR spectrometer (BOMEM DA2.16) - Sample and BB furnaces - Transient measurement	500-1000	2-22	KBO_2, $NaBO_2$, B_2O_3, $LiBO_2$	1 % at 20 μm 5 % at 2μm
[85]	- High-speed spectrometer - Graphite furnace - Induction coil - Vacuum chamber - Steady-state measurement	727-1527	1.5-5.5	"White" and "black" borosilicate coating on silica glass	1 % and 4 % for random and systematic errors, respectively
[38]	- FTIR spectrometer - vacuum chamber - blackbody cavity - Mikron ratio pyrometer	1167, 1215, 1278, 1332	1-16	High-purity nickel	< 4 % at 1167 °C and λ = 1 μm
[86]	- Vacuum IR standard radiation thermometer (VIRST) - Vacuum FTIR spectrometer (Bruker Vertex 80V)	0-430	1-1000	-	-
[87]	- FTIR spectrometer - Vacuum chamber	-40-450	4-100	SiC, gold mirror	< 1 %
[88]	- FTIR spectrometer - main (Isotech R970) and assisted BB - sample chamber - electrical heater	400-1200	2-25	SiC samples	< 2.6 % at 1200°C

Table 3. Summary of direct emissivity measurement systems by using the FTIR spectroscopy (part 2)

Reference	Measurement methods and devices	Temperature range (°C)	Spectral range (μm)	Materials	Experimental error
[5]	- High-resolution FT spectrometer - Vacuum chamber with periscope, shutter, graphite heater block and water-cooled furnace	150-1800	0.6-9.6	Boron nitride (BN), Fecralloy steel, and polished tantalum (Ta) samples	3 % - 10 %
[20], [89], [90]	- High Accuracy Homemade Infrared Radiometer (HAIR): - FTIR spectrometer (Bruker IFS66v/S) - Vacuum chamber - Controlled environment	200-650 330-730 200-800	2-22	Inconel 718, René 41, and Haynes 25 (aeronautical alloy). Atmospheric plasma sprayed yttria stabilized zirconia (YSZ) films layered on Inconel 718 substrates Set of solar-absorbing layers based on Cu-alloyed spinel nanoparticles	-
[91]	- FTIR spectrometer - BB (Systems SR-2) - Controlled environment	227-927	2.5-20	HfC and TaB_2 ultra-refractory ceramic samples	± 20 % at 2.7 μm ± 10 % in the remaining bands
[92]	- FTIR (Michelson type) - BB plates - Pt100 sensors	≈120	3-5	Sheathing used in vehicles	± 5 % (ε panel) ± 2 % (ε BBs)
[93]	- FTIR (Michelson type) - Cool-water system - SiC heater with a black hole	60-1500	0.6-2.5	low and high reference BBs	< 3 %
[29]	- self-made infrared radiometer based on FT-IR spectrometer - blackbody radiator	700	3-20	TiO_2 coatings on titanium alloy surface (ceramic coatings) and uncoated titanium sample	< 5 %
[33]	- Perkin-Elmer Model 13 spectrometer - Hohlraum - Emission furnace - In air environment	605±8	1.2-14.1	ZnO, Al_2O_2 on opaque substrate	± 3 %
[34]	- FTIR spectrometer (FTS-60A/596) - Vacuum chamber - Cooling shroud - thermopile module with the Christiansen effect filter	500-700	1.60-22	Zirconia (ZrO_2)	-
[41]	- Two-substrate heating	300-350	2.5-25	Alumina on two substrates	< 4.3 % at 4 μm < 0.57 % at 10 μm
[94], [35]	- Fast Infrared Array Spectrometer (FIAS) - Multispectral Radiation Thermometry (MRT) models	327,427,527	2.05-4.72	Polished aluminium alloy samples	-
	-			Roughened aluminium alloy samples	-
[36], [37]	- Fast Infrared Array Spectrometer (FIAS) - Multispectral Radiation Thermometry (MRT) models	427,527,627	1.2-4.8	Stainless and tool steel samples	Temp. prediction errors < 10 % (In certain conditions < 1 %)
	-				Half of the temp. prediction errors < 10 % (randomly < 1 %)

Lindermeir et al. [92] proposed the simultaneous measurement of emissivity and surface temperature of opaque materials heated independently, using a Michelson-type spectrometer. Thus, a calibration procedure was investigated to reduce the influence of high irradiation from the surroundings (i.e., radiance from the atmosphere, optical, and electronic components). However, the measured spectral and temperature ranges were limited to 3-5 μm and 100 °C above ambient temperature. At HIT, a water-cooled chamber and a SiC heater with a black hole were designed for heating two blackbodies at higher temperatures (up to 1500 °C),resulting in an emissivity measurement uncertainty lower than 3 % [93]. However, the methods described in the last two papers are limited to opaque materials. To overcome this limitation, different researchers have exploited FTIR spectrometry to focus their investigations on the radiant behaviour of semi-transparent materials at high temperatures [29], [30], [33], [34], [41], [40]. In particular, a "two-substrate heating" method was investigated by Lee et al. to overcome parasitic radiation due to the substrate and simultaneously measure normal and directional spectral emittance [41].

Some researchers have investigated the possibility of adopting a heating system without a confined surrounding (e.g., laser heating) to reach very high temperatures. In particular, Sova et al. [82] proposed using carbon dioxide (CO_2) laser heating to obtain the optical properties of various oxides at very high temperatures (above 4227 °C). However, non-uniform heating caused high thermal gradients between the centre and the edges of the sample. To overcome this issue, Rozenbaum et al. [83] reduced the thermal gradients by heating oxide materials more homogeneously, up to 2727 °C, with the CO_2 laser beam split into two equal parts. Good uniformity of thermal heating was ensured in [84] by utilizing an isothermal furnace, heating the samples (poorly conductive and highly transparent powdered materials) above the melting point (1000 °C) to obtain flat

surfaces, and then quickly removing the samples and performing the measurement (processing time: ≤ 1 s). As a result, the thermal gradient within the samples was very low (1.7 °C/cm at 727 °C). Recently, Pierre et al. used laser heating to simultaneously measure the temperature and emissivity of metals above their melting point [95]; They used a six-wavelength pyrometer within an approach based on both deterministic and Bayesian techniques. However, they stressed the necessity to couple their methodology with considerations on temperature-emissivity separation. Nonetheless, other sources of error were found to be linked to the high-speed cooling of the samples and absorption along the optical path, partially reduced in [85] with a high-speed spectrometer and by keeping the path lengths to the calibration blackbody and the sample surface equal. More recently, it was demonstrated that the use of a vacuum chamber allows for smaller uncertainties (< 1 %) compared to air, avoiding undesired thermal radiations exchanged with the atmosphere [86], [87]. In addition, the vacuum chamber also minimizes undesired material chemical processes, such as oxidation phenomena. In [34], a new apparatus for simultaneous measurements of normal spectral emissivity, optical constants, and material thickness was proposed for ceramic samples. In particular, a thermopile module with the Christiansen effect filter defined the wavelength at which the spectral reflectivity of each investigated material was zero, leading to an accurate measurement of surface temperature and, consequently, specimen emissivity. An improved algorithm based on the modified two-temperature calibration method was proposed in [88] to eliminate disturbances and enhance the measurement accuracy of emissivity. This method allowed calibrating the system using the main blackbody (Isotech R970), while an assisted blackbody was adopted to compensate for the offset for the drift of the background radiation and the zero-point deviation of the FTIR spectrometer. The reliability of the improved algorithm and the experimental apparatus was verified on a SiC sample, obtaining a combined uncertainty lower than 2.6 % at 1200 °C, except for the spectral bands of atmospheric absorption (4.8-8 μm). Most of the above-mentioned studies describe methods for normal emissivity measurements, except in [36], where measurements were limited to the viewing direction from normal to 50°. On the other hand, different laboratory prototypes were developed and tested for the characterization of directional-spectral emissivity as a function of temperature and emission angle, with a particular focus on high-temperature applications in controlled environments [20], [28], [89], [91], [75]. In particular, the MEDIASE facility used in [28] reproduced the conditions expected near the sun and enabled directional emissivity measurements from normal up to 80°. In [76], a modified Fabry–Perot resonator, characterized by a layered structure, was designed for directional-spectral emittance measurements at a given polarization and temperatures up to 527 °C. The emittance peaks in the cavity resonator become broader with increasing temperature, and the resonance frequencies slightly shift to lower wavenumbers. Niu et al. developed a new technique to measure the emissivity in an arbitrary direction in the 27-1500 °C temperature range [77]; the FTIR spectrometer was used as a radiation detector in the normal direction, while a Stochastic Particle Swarm Optimization (SPSO) algorithm was adopted as an inverse method to predict the apparent spectral directional emissivity from the refractive index and absorption coefficient retrieved before, obtaining good agreement with experimental results. More recently, different researchers explored the use of optical fibre-spectrometry for its greater portability, wider flexibility, and lower cost. In particular, a new experimental apparatus was developed and evaluated in [78] to perform emissivity measurements in the NIR band. Recent studies also focus on the use of a fibre-optic spectrometer system combined with image processing techniques for temperature and spectral emissivity measurements of air combustion flames, generally assumed as grey sources for the close wavelength range (0.2-1 μm). The radiant properties of solid fuel particles find significant interest in furnace applications, improving combustion efficiency or minimizing pollution. In [79], a portable fibre-optic spectrometer was combined with the two-colour method to measure the temperature and emissivity of a pulverized coal flame. In [80] the same spectrometer was used simultaneously with a high-speed camera for the transient response of spectral emissivity of an R-type thermocouple, subjected to either steady or unsteady flame of a Bunsen burner. The thermocouple was heated at four different flame conditions (by varying the fuel/air equivalence ratio) up to 1257 °C, and the results showed the ability of this method to measure varying temperature and emissivity. Zheng et al. [81] performed in situ temperature and emissivity measurements of three different biomasses using the multi-wavelength radiation thermometry method and a fibre-optic spectrometer. The flame emission spectrum was obtained for the temperature range 1130-1330 °C and spectral range 0.4-0.9 μm, showing the same trend in the results: the emissivity decreases as the wavelength increases.

3.2.2. Thermography

Thermography, or infrared imaging, is a widely used non-contact measurement technique for scanning infrared regions of surface objects over a wide temperature range (typically from -20 °C up to 1500 °C). An infrared system is characterized by a thermal camera equipped with fixed/changeable lenses, providing a quantitative temperature map of the tested sample/environment. Table 4 summarizes different works exploiting radiometric methods based on the use of a thermal camera.

Different thermal and spectral sensitivities are provided depending on the detection technologies adopted in the studies. For example, photon detectors are used if high sensitivity response is required at a specific wavelength, while a microbolometer detector is a low-cost detector more suitable for long-term use. In [104] an accuracy of 0.005 in the measured emissivity was obtained for emissivity values ≥ 0.92 with the AGA Thermovision System 680 by using a single InSb detector at 5 μm to assess the apparent emissivity of a black painted hood at ambient temperature. Inagaki and Okamoto used an IR camera with different sensitivities at three different detection wavelength bands, employing In-Sb (25 μm), Hg-Cd-Te (69 μm), and Hg-Cd-Te (8~13 μm) sensors for detecting the two-dimensional temperature distribution of non-metal surfaces, demonstrating the dependence of their radiation properties on wavelengths [107]. Furthermore, Chrzanowski proposed a new formula for determining more accurate effective emissivity by using photon detectors with variable spectral sensitivity [108].

More recent cameras are characterized by multiple detectors arranged in a matrix and characterize the focal plane array (FPA) that provides higher sensitivity [97], [98]. Generally, a blackbody with known emissivity or a thermocouple can be used as reference for emissivity estimation [104], [105], [102]. On the other hand, Especel and Mattei demonstrated that the emissivity can also be measured without a reference [109]. In particular, a modulated IR source was proposed for simultaneous emissivity

Table 4. Summary of direct emissivity measurement systems by using thermal camera.

Reference	Measurement methods and devices	Temperature range (°C)	Spectral range (μm)	Materials	Experimental error
[96]	- IR camera - platinum resistance thermometer (PRT) - temperature-controlled brass sample holder - conical water-bath IR blackbody (CASOTS)	19-45	7.5- 13	Microwave absorbing, material loaded with different concentrations of carbonyl iron powder (CIP)	3.3 %
[97]	- IR camera (FLIR S40) - IR camera (FLIR S2000)	up to 1100	7.5- 13	Etnean basalt	< 1 % (instrument error)
[98]	- IR camera with microbolometer uncooled Focal Plane Array (FPA) - IR reflector	40-550	7.5-13.5	aluminium nitride plat	< 5 % in absolute value < 1 % dispersion over the entire T range
[27]	- IR camera (CEDIP) - Vacuum vessel - radiant and electron bombardment heater - K-type thermocouple	200–850	1.7–4.75	tungsten plasma facing components	-
[99]	- InGaAs photodiode detector - eddy current heater - 2 platinum-rhodium thermocouples	527-827	1.5	*Steel 201*	3.2-14.1 %
[100]	- Nd:YAG laser emitted light pulses - IR camera	27-87 27-177	1.5-5	nickel sheet AISI 304 stainless steel sheet	18 % (expanded uncertainty, k = 2)
[101]	- AGEMA type 570 IR-camera - Blackbody	Up to 727	7.5-13	3 different pool diameters with oil and gasoline	-
[102]	- IR-camera - Blackbody - Two thermocouples - Two video cameras	Up to 1327	7.5-13	Forest fuel: Pinus halepensis Rosmarinus officinalis	-
[103]	- Airborne thermal images - LIDAR data - GIS data - IUEM-SVF model	55 (rooftop) 43.5 (street) 32 (wall)		Concrete and cement (materials of buildings)	
[104]	- IR camera (AGEMA) - Black paint epoxy - Specular hemisphere	37-120	3-5	Metallic (bronze), insulating (glass) powders and their mixtures	Mean error of 3 %
[105]	- IR camera (FLIR T 400) - Emissometer - Black tape (Scotch® 3M +33 Super)	70	7.5-13.0	Autoclaved aerated concrete (AAC), stainless steel, gypsum, mortar, ceramic tile, pine wood, limestone, granite, solid brick and cork	Average differences with the emissometer of 3.4 % (ε values from 0.82 to 0.94)
[106]	- AGA camera system 680 - Heimann KT4 radiation thermometer	Ambient temperature	5, 10	Leaves of tree or green plants, wood, plastics, paper, human skin, and some other materials	0.005
[107]	- IR camera with three detection wavelength bands - Blackbody wall	20-100	2-13	Various non-metal surfaces made of graphite, mortar, carbon composite fibre (CCG) and SiC.	-
[108]	- IR detector systems - blackbody	227-527	3-5	Brick and titanium	-
[109]	- IR source and pyroelectric detector - thermocouples	Ambient temperature	1-50	Black paint, duralumin and aluminium paint	-
[110]	- IR camera (FLIR SC3000)	227-627	3.6-5.0	Fused quartz	
[6]	- Wide-band infrared sensor (RM-6A) - collimation tube - K-type thermocouple blackbody furnace	100-500	2-16	Stainless steel coated with a black coating or with a high emissivity coating; brass	< 0.05

and reflectivity measurements via periodic radiometry, and the validity of the method was proved on different samples near ambient temperature. At higher temperatures, McDaid proposed an iterative method to demonstrate that even a slight change in temperature distribution might cause large variations in radiation heat loss [110]. The emissivity dependence on viewing angle above 75° was also shown. More recently, Chen et al. proposed a new in situ online method based on thermal imager for estimating emissivity at temperatures up to 500 °C [6], ensuring an emissivity uncertainty within 0.05 (in the temperature range from 313 K to 823 K) by a new blackbody equivalent verification. Different materials were investigated exploiting thermography. Thermal properties of microwave-absorbing samples, with varying iron carbonyl powder concentrations, were investigated in [96], being very useful as microwave radiometer calibration sources. In [97], results on basaltic lava emissivity

were presented; in particular, the instrument error and external factors influencing measurement accuracy (e.g., viewing angle) were analysed. In [27] the dependence of a low-emissivity material (tungsten plasma-facing components) on wavelength, temperature, and surface state was demonstrated (emissivity increases with increasing temperature, whereas it decreases with increasing wavelength). A screen inside the vacuum vessel was positioned to avoid reflections on the top of the surface that might highly influence a low-emissivity material. The utility of using the vacuum chamber for minimizing oxidation phenomena in materials under heating exposure, whose effects on spectral emissivity measurements are quantified for steel 201, was described in [108]. The measurements' dependence on other characteristics of the surface specimen (e.g., roughness, thickness, etc.) was also addressed by researchers, as in Jeromen et al. [100]. Another field of interest at high temperature is related to the assessment of radiation emitted from a flame, which strongly depends on the different particles involved in combustion. In [101], the flame transmissivity was calculated to obtain the emissivity of turbulent pool fires; the IR camera was positioned at three different locations with respect to the specimen and the blackbody to measure the incident radiation. In the experimental setup adopted by Pastor et al. [111], two video cameras and two thermocouples were utilized in addition to the IR camera.

3.2.3. Radiation thermometer

Even though the current technology of thermal imaging cameras allows for higher resolution images, radiation thermometers, i.e., pyrometers, still represent the most commonly used instruments when focused optics are sought. Table 5 lists some research that adopts radiation thermometers. Different sensitivities to temperature measurements, and consequently to spectral emissivity, can be achieved by using pyrometers that exploit one, two, or more wavelengths. In particular, a single-color pyrometer is adopted when higher sensitivity is required in a carefully chosen selected waveband. On the other hand, two or more colour pyrometers are characterized by thermal detectors that respond to the radiation emitted at two or more selected wavelengths in an equivalent

Table 5. Summary of direct emissivity measurement systems by using radiation thermometer

Reference	Employed measurement methods and devices	Temperature range (°C)	Spectral range (μm)	Materials	Experimental error
[112]	- narrow bandwidth pyrometer (Impac IGA 5-LO MB25)	477-277 477-1057	1.45 - 1.8	Hot titanium alloy	Relative uncertainty in temperature < 2.5 %
[113]	- Single color pyrometers (IMPAC IGAR12LO, MIKRON -M76S, -M67S) - Thermocouple (K-type) - Blackbody cavity	450-850°C (IGAR12-LO) 400-800°C (M76S) 650-850°C (M67S)	1.52-1.64 (IGAR12-LO) 1.00-1.16 (M76S) 0.78-1.06 (M67S)	OFHC copper	< 3 % (at 657 °C - IGAR12-LO) < 3 % (at 462 °C - M76S) ≈ 0 % (M67S)
[114]	- Linearpyrometer LP2 - Thermoelectric micro-sensor - Blackbody hole	800-1300	0.5-0.9 (Linearpyrometer) 1.3-8.3 (thermal detector)	Three standard coating: OT13 ATZ and STZ	
[115]	- Linearpyrometer LP2 - Thermoelectric micro-sensor - Blackbody hole	700- 1313	0.5-0.9 (Linearpyrometer) 1.3-8.3 (thermal detector)	Two high-emissivity paints (HE6 and HE23)	A table of different uncertainty contribution is provided
[82]	- Vacuum emissometer (with BOMEM DA3.02 spectrometer) - CO2 laser heating - Two-colour pyrometry technique	527-1727	2-20	Oxides: sapphire, spinel, yttria, aluminium oxynitride, fused silica	-
[116]	- Two-colour pyrometer (Model H322) - COMSOL simulation (heat transfer)	≈ 977-1477	1.65-1.80 (1st channel) 1.40-1.65 (2nd channel)	Stainless steel 316L powder	Approximately 1 % error between simulated and measured temperature
[117]	- fast fiber-optic two-colour pyrometer	up to 300	1.70, 2.0	Different metallic surfaces	Absolute temperature error < 2 % at 727 °C
[118]	- fluoride glass optical fiber - two HgCdTe detectors equipped with bandwidth filters	200-800	2.55-3.9	Brake disk	< 0.21 and 0.15 for temperatures Higher than 300 °C and 350 °C respectively
[4]	- Pyrometer and IR camera - Thermocouple - Blackbody - Solar furnace SF5	600-1000	1.4 (pyrometer) 1.5-5 (IR camera)	Stainless steel	Repeatability (1 %) and accuracy (< 2 %)
[7], [119]	- Laser-flash apparatus: high energy pulsed laser, high temperature furnace and radiation thermometer	2727	1.06	Tungsten	Arithmetic error < 1 %
		627-1827		Isostatic-pressed graphite	± 5 %
[120]	- Black (Vantablack®) and gold coated cup - custom designed radiation thermometer - Hot plate and data acquisition system - blackbody furnace (for calibration)	200 - 450	2.1- 2.5	Aluminium alloy 6082, stainless steel 304, HiE-Coat 840-M paint	< 0.058

way, provided that these wavelengths are very close to each other.

The ratio of the output voltages related to the different wavelengths is a function of temperature but is not dependent on emissivity anymore. Hagqvist et al. proposed a narrow-bandwidth radiation pyrometer (1.45-1.8 μm) for a versatile procedure to assess the spectral emissivity of titanium alloy (Ti-6Al-4V) at high temperatures [112]. Purpura et al. tested three different types of single-color pyrometer models (by IMPAC-IGAR 12LO and MIKRON-M67S) at different temperature ranges, up to 850 °C [113]. The experimental results were verified using a semi-empirical formula and obtaining a maximum error of less than 3 % for all three models. In addition, a preliminary CFD analysis was also conducted to verify the uniform temperature distribution on the sample inside a graphite spherical cavity. Neuer et al [114] used a linear pyrometer LP2 [120], [121] with interference filters and a thermoelectric micro-sensor, both measuring over a small drill hole to perform high-temperature measurements of different high-emissivity coatings. However, Brandt et al. demonstrated that the main contribution of emissivity uncertainty obtained by using this configuration was due to the integrated temperature measured over the hole depth [109]. Regarding two-colour pyrometry, many researchers have developed strategies for high-temperature applications. Sova et al. combined the technique with an FTIR spectrometer and a vacuum chamber to obtain the emissivity of some oxides at temperatures in the range of 327-1727 °C [82]; the sensitivity of the instrumentation for temperature surface measurement decreased with increasing temperature. At higher temperatures, the multiphoton edge technique can be used in conjunction.

More recently, a two-colour pyrometer was used to investigate the emissivity of stainless steel 316L powder at 977-1477 °C at two different spectral ranges: 1.65-1.80 μm (1st channel) and 1.40-1.65 μm (2nd channel) [116]. An error of approximately 1 % was obtained between a numerical heat transfer simulation and the temperature measured. Optical filters can also be integrated into radiation thermometers. Muller and Renz adopted quartz fibres to enable temperature measurements up to 300 °C on low-emissivity materials, providing high spatial and temporal resolution at locations with limited optical access [117]. A particular focus was on the system adopted to separate the two wavelength bands, i.e., the dichroic beamsplitter, which offers advantages in terms of efficiency and ease of use compared to the filter wheel, as used in [2]. Thevenet et al. used a fluoride glass optical fibre equipped with a two-colour IR device for measuring the temperature and the emissivity of a brake disc surface that constantly changes during the test [112]. A novel approach to performing measurements at higher temperatures up to 2727 °C was proposed by Krenek et al., who designed a commercial laser flash apparatus for measuring emissivity dynamically changing [119]. The specimen is heated by an optical pulse, while a radiation thermometer (LP5HS) provides the resulting fast temperature rise of the specimen under test. The main uncertainty sources are linked to the radiation correction of the hot surrounding furnace, the temperature-dependent heat capacity of the specimen, the laser energy measurement, and the numerical fit applied to determine the adiabatic temperature rise from the observed data. More recently, a new instrument for obtaining direct, indirect, and in-situ measurements was proposed by Zhu et al. [120]; the new apparatus is mainly characterized by a custom-designed radiation thermometer and a pair of hemispherical cups (gold and black) to obtain emissivity measurements of low-, middle-, and high-emissivity materials.

4. CONCLUSIONS

When approaching high-temperature emissivity measurements involving non-contact technologies, researchers need to consider the accuracy and the advantages or drawbacks of each solution they are willing to use. This section discusses the main characteristics and limitations of the different methodologies reported in the previous sections. In general, the main advantage of indirect methods is the possibility to determine emissivity in the near-infrared and visible (VIS) spectra because of the higher radiation intensity below the wavelength of 3 μm at moderate temperature values. On the contrary, at higher temperatures and wider spectral range, technical issues arise due to higher background noise levels and because transmission becomes increasingly specular. Moreover, their applicability is more widespread for opaque materials rather than for semi-transparent ones at high temperatures; for these reasons, semi-transparent materials are usually measured with indirect methods only at ambient temperature. In addition, thin multi-layer samples are difficult to measure, being subjected to multiple reflections.

Regarding direct emissivity measurements, it is worth mentioning that a significant signal-to-noise ratio (SNR) at short wavelengths can be obtained only at very high temperatures; hence, solutions working in the medium- and long-IR regions are more effective. At temperatures below 300°C, measurements are more influenced by the radiation reflected from the surrounding environment. Indeed, this radiation may be difficult to filter out. Finally, indirect methods are more indicated for measuring low-emissivity materials, whereas direct methods are more suitable for all the others. Among the direct methods, calorimetry performs measurements in the overall radiation for all wavelengths and all directions, while the others are limited in terms of spectral range or direction (or both). However, this is also a limitation when spectral and directional emissivity measurements are required. Another issue, common to all the direct radiometric methods, is related to the need for thermal insulation of the investigated specimen from the surroundings. Calorimetric apparatuses are conceptually simple, and their cost is relatively low; in addition, the use of blackbodies is not required, even if a vacuum chamber is necessary to avoid heat transfer by conduction and convention.

FTIR spectrometry is the most suitable method for accurately measuring both total and directional emissivity. High-temperature applications require stable measurement conditions to improve sensitivity and SNR: the use of vacuum chambers, blackbody cavities, and the different designs of the heating systems allow the reduction of errors due to uneven temperature distribution, influence of the surrounding radiation, and undesired chemical reactions on the material surface. However, the confined small size of the sampling chamber and the heavy instrumentation are some of the causes that limit the use of this approach. Wide-band infrared sensors typically replace the use of precision instruments, such as FTIR spectrometers, in industrial applications. Thermal cameras allow providing the temperature distribution of large areas. However, the viewing angle and the lenses of the thermal camera should be chosen to minimize the effect of directional emissivity; in fact, the angular distribution of emissivity is neglected when the camera viewing angle is set at 45° to the normal [122]. Other possible sources of error include: a) radiation reflected from the surrounding environment, which can be partially reduced by using black body cavities; b) temperature gradients due to variations in the

characteristics of the examined surface. These risks can be avoided by using pyrometers with focusing optics. However, the wavelength characterizing the pyrometer should be tailored to the temperature range of interest and the material investigated.

From a metrological point of view, it is important to underline a lack of standardized approaches in the literature, both in terms of test protocols and reference instrumentation:

- Test protocol: Researchers have developed a variety of test protocols targeting specific applications. Any other material not covered by the literature might need its own specific measurement procedure. This is costly in terms of time and effort and is also risky, as many factors could negatively influence the measurement results in a brand-new testing protocol.
- Reference instrumentation: The reference technology can vary greatly, as can the accuracy of the testing approach adopted as a reference. This represents an important aspect in the definition of the measurement chain in the test protocol.

These aspects may cause inhomogeneities, resulting in results that are barely comparable, also because measurement uncertainty is not always defined according to metrology standards [123], [124]. However, despite these drawbacks, it is important to underline that the literature targeting emissivity characterization at high temperature can indeed provide several useful recommendations for different application fields, which is extremely supportive when designing a measurement chain. In particular, there are three grounding rules that should always be considered:

- Consider the target operating temperature to be reached during the test and its homogeneous distribution on the sample surface;
- Do not forget the radiant properties of the investigated sample and its morphology, thickness, and surface roughness/finishing;
- Try to reduce oxidation phenomena by using vacuum chambers whenever possible or adopting suitable heating/cooling times that do not allow these phenomena.

Authors believe that it might be possible to use these rules as a basis towards the creation of standards regulating the measurement of material emissivity at high temperature, ensuring appropriate consideration of measurement uncertainty-related aspects.

ACKNOWLEDGEMENT

This research was funded by the European Union Horizon 2020 research and innovation programme under grant agreement number 820783 (DESTINY project).

REFERENCES

[1] J. Hartmann, High-temperature measurement techniques for the application in photometry, radiometry and thermometry, Physics Reports, vol. 469, no. 5–6, Jan. 2009, pp. 205–269. DOI: 10.1016/j.physrep.2008.09.001

[2] E. R. Woolliams, G. Machin, D. H. Lowe, and R. Winkler, Metal (carbide)–carbon eutectics for thermometry and radiometry: a review of the first seven years, Metrologia, vol. 43, no. 6, Nov. 2006, pp. R11–R25. DOI: 10.1088/0026-1394/43/6/r01

[3] B. Yang, S. Z. W. Zhang, M. Li, L. Yang, Steady-state Calorimetry Measurement Method for Total Hemispherical Emissivity of Thermal Insulating Coating, IOP Conf. Series: Earth and Environmental Science, vol. 170, n. 4, 2018, p. 04. DOI: 10.1088/1755-1315/170/4/042105

[4] J. Ballestrín, J. Rodríguez, M. E. Carra, I. Cañadas, M. I. Roldan, Pyrometric Method for Measuring Emittances at High Temperatures, AIP Conf. Proc., vol. 1734, 2016, p. 130003. DOI: 10.1063/1.4949213

[5] B. Zhang, J. Redgrove, J. Clark, New apparatus for measurement of the spectral, angular, and total emissivity of solids, High Temperatures - High Pressures, vol. 36, n. 3, 2004, pp. 289-302.

[6] X. Chen, L. Ye, Z. Zhu, K. Gui, H. Zhang, An in situ online methodology for emissivity measurement between 100 °C and 500 °C utilizing infrared sensor, Infrared Physics and Technology, vol. 102, 2020, p. 102974. DOI: 10.1016/j.infrared.2019.102974

[7] S. Krenek, D. Gilbers, K. Anhalt, D. R. Taubert, J. Hollandt, A Dynamic Method to Measure Emissivity at High Temperatures, Int. Journal of Thermophysic, vol. 36, 2015, p. 713–1725. DOI: 10.1007/s10765-015-1866-7

[8] Z. Yi, W. J. Zhang, Q. D. Yang, G. J. Li, H. G. Chen, Influence analysis of the furnace wall emissivity on heating process, Infrared Physics and Technology, vol. 93, 2018, pp. 326-334. DOI: 10.1016/j.infrared.2018.08.009

[9] E. Sani, L. Mercatelli, F. Francini, J.-L. Sans, D. Sciti, Ultra-refractory ceramics for high-temperature solar absorbers, Scripta Materialia, vol. 65, 2011, pp. 775-778. DOI: 10.1016/j.scriptamat.2011.07.033

[10] L. d. Campo, R. Pérez-Sáeza, L. González-Fernándeza, X. Esquisabelc, Emissivity measurements on aeronautical alloys, Journal of Alloys and Compounds, vol. 93, 2010, p. 482–487. DOI: 10.1016/j.jallcom.2009.09.091

[11] G. Neuer, G. Jaroma-Weiland, Spectral and Total Emissivity of High-Temperature Materials, Int. Journal of' Thermophysic.i, vol. 19, 1998. DOI: 10.1023/A:1022607426413

[12] G. Machin, K. Anhalt, F. Edler, J. V. Pearce, M. Sadli, R. Strnad and E. M. Vuelban, HiTeMS: A project to solve high temperature measurement problems in industry. AIP Conf. Proc., 2013. DOI: 10.1063/1.4821414

[13] H. C. McEvoy, D. H. Lowe, R. Underwood, M. de Podesta, G. Machin, M.J. Martin, J.M. Mantilla, J. Campos, M. Sadli, F. Bourson, S. Briaudeau, R. Salim,, K. Anhalt, M. Waehmer, D. R. Taubert, X. J. Feng, J. T. Zhang, X. F. Lu, H. Yoon, Methodologies and uncertainty estimates for T – T 90 measurements over the temperature range from 430 K to 1358 K under the auspices of the EMPIR InK2 project. Measurement Science and Technology, 2020. DOI: 10.1088/1361-6501/abc50f

[14] A. S. Lavine, F. P. Incropera, D. P. DeWitt, T. L. Bergman, Fundamentals of heat and mass transfer, 8th Edition, 2018, Wiley.

[15] J. Jones, P. Mason, A. Williams, A compilation of data on the radiant emissivity of some materials at high temperatures, Journal of the Energy Institute, vol. 92, 2019, pp. 523-534. DOI: 10.1016/j.joei.2018.04.006

[16] J. Hartmann, Y. Joumani, B. Hay, R. Razouk, K. Anhalt, S. Sarge, J. Wu, N. Milosevic, M. Cataldi, C. Lorrette, K. Boboridis, J. Manara, S. Vidi, P. Pichler, T. Denner, EMPIR Hi-TRACE project – Metrological facilities for measuring thermophysical properties up to 3000 °C, Tempmeko 2019, Chengdu, China.

[17] J. Song, X. P. Hao, Z. D. Yuan, Z. L. Liu, L. Ding, Research of Ultra-Black Coating Emissivity Based on a Controlling the Surrounding Radiation Method, Int. Journal of Thermophysics, vol. 39, 2018, pp. 1-10. DOI: 10.1007/s10765-018-2404-1

[18] E. Stamate, Transparent and low emissivity coatings based on aluminum doped zinc oxide, 4th Int. Workshop on Solution Plasma and Molecular Technologies., 2016.

[19] P. Honnerová, J. Martan, Z. Veselý, M. Honner, Method for emissivity measurement of semitransparent coatings at ambient temperature, Scientific reports, vol. 7, n. 1, 2017, pp. 1-14. DOI: 10.1038/s41598-017-01574-x

[20] L. González-Fernández, L. d. Campo, R. Pérez-Sáez, M. Tello, Normal spectral emittance of Inconel 718 aeronautical alloy coated with yttria stabilized zirconia films, Journal of Alloys and Compounds, vol. 513, 2011, pp. 101-106.
DOI: 10.1016/j.jallcom.2011.09.097

[21] D. Cardenas-Garcıa, Emissivity measurement of high-emissivity black paint at CENAM, Revista Mexicana de Fısica, vol. 60, 2014, p. 305–308.

[22] P. Honnerova, J. Martan, M. Honner, Uncertainty determination in high-temperature spectral emissivity measurement method of coatings, Applied Thermal Engineering, vol. 124, 2017, pp. 261-270.
DOI: 10.1016/j.applthermaleng.2017.06.022

[23] S. Meng, H. Chen, J. Hu, Z. Wang, Radiative properties characterization of ZrB2–SiC-based ultrahigh temperature ceramic at high temperature, Materials and Design, vol. 32, 2011, pp. 377-381.
DOI: 10.1016/j.matdes.2010.06.007

[24] G. Cao, S. J. Weber, S. O. Martin, T. L. Malaney, S. R. Slattery, M. H. Anderson, K. Sridharan, T. R. Allen, In situ measurements of spectral emissivity of materials for very high temperature reactors, Materials for Nuclear Systems, vol. 175, 2010, pp. 460-467.
DOI: 10.13182/NT11-A12317

[25] C. Y. Peng, X. G. Yue, G. T. Chao, Z. Ning, Infrared emissivity and microwave absorbing property of epoxy-polyurethane/annealed carbonyl iron composites coatings, Sci China Tech Sci, vol. 55, n. 3, 2012, p. 623–628.
DOI: 10.1007/s11431-011-4696-2

[26] T. Fu, P. Tan, M. Zhong, Experimental research on the influence of surface conditions on the total hemispherical emissivity of iron-based alloys, Experimental Thermal and Fluid Science, vol. 40, 2012, pp. 159-167.
DOI: 10.1016/j.expthermflusci.2012.03.001

[27] J. Gaspar, C. Pocheau, Y. Corre, N. Ehret, D. Guilhem, M. Houry, T. Loarer, T. Loewenhoff, C. Martin, C. Pardanaud, G. Pintsuk, M. Richou, F. Rigollet, H. Roche, G. Sepulcre, M. Wirtz, Emissivity measurement of tungsten plasma facing components of the WEST tokamak, Fusion Engineering and Design, vol. 149, 2019, p. 111328.
DOI: 10.1016/j.fusengdes.2019.111328

[28] E. Brodu, M. Balat-Pichelin, J.-L. Sans, J. Kasper, Influence of roughness and composition on the total emissivity of tungsten, rhenium and tungstenâ€25% rhenium alloy at high temperature, Journal of Alloys and Compounds, vol. 585, 2014, pp. 510-517.
DOI: 10.1016/j.jallcom.2013.09.184

[29] Z. Wang, Y. Wang, Y. Liu, J. Xu, L. Guo, Y. Zhou, J. Ouyang, J. Dai, Microstructure and infrared emissivity property of coating containing TiO2 formed on titanium alloy by microarc oxidation, Current Applied Physics, vol. 11, 2011, pp. 1405-1409.
DOI: 10.1016/j.cap.2011.04.011

[30] X. He, Y. Li, L. Wang, Y. Sun, S. Zhang, High emissivity coatings for high temperature application: Progress and prospect, Thin Solid Films, vol. 517, 2009, p. 5120–5129.
DOI: 10.1016/j.tsf.2009.03.175

[31] H. Tanaka, S. Sawai, K. Morimoto, K. Hisano, Evaluation of Hemispherical Total Emissivity for Thermal Radiation Calorimetry, Int. Journal of Thermophysics, vol. 21, 2000, n. 4, pp. 927-940.
DOI: 10.1023/A:1006670409740

[32] H. Masuda, S. Sasaki, H. Kou, H. Kiyohashi, An Improved Transient Calorimetric Technique for Measuring the Total Hemispherical Emittance of Nonconducting Materials (Emittance Evaluation of Glass Sheets), Int. Journal of Thermophysics, vol. 24, n. 1, 2003, pp. 259-276.
DOI: 10.1023/A:1022378602663

[33] C. Liebert, Spectral emittance of aluminum oxide and zinc oxide on opaque substrates. National Aeronautics and Space Administration, 1965, pp. 1-22.

[34] K. Nakazawa, A. Ohnishi, Simultaneous measurement method of normal spectral emissivity and optical constants of solids at high temperature in vacuum, Int. Journal of Thermophysics., vol. 31, 2010, p. 2010–2018.
DOI: 10.1007/s10765-010-0847-0

[35] C. D. Wen, I. Mudawar, Emissivity characteristics of roughened aluminum alloy surfaces and assessment of multispectral radiation thermometry (MRT) emissivity models., Int. Journal of Heat and Mass Transfer, vol. 47, 2004, p. 3591–3605.
DOI: 10.1016/j.ijheatmasstransfer.2004.04.025

[36] C. D. Wen, Investigation of steel emissivity behaviors: Examination of Multispectral Radiation Thermometry (MRT) emissivity models, Int. J. Heat Mass Transfer, vol. 53, 2010, p. 2035–2043.
DOI: 10.1016/j.ijheatmasstransfer.2009.12.053

[37] C. D. Wen, Study of steel emissivity characteristics and application of multispectral radiation thermometry (MRT), Journal of materials engineering and performance, vol. 20, 2011, p. 289–297.
DOI: 10.1007/s11665-010-9666-5

[38] G. Teodorescu, P. Jones, R. Overfelt, B. Guo, Normal emissivity of high-purity nickel at temperatures between 1440 and 1605K, Journal of Physics and Chemistry of Solids, vol. 69, 2008, p. 133–138.
DOI: 10.1016/j.jpcs.2007.08.047

[39] F. Zhang, K. Yu, K. Zhang, Y. Liu, K. Xu, Y. Liu, An emissivity measurement apparatus for near infrared spectrum, Infrared Physics & Technology, vol. 73, 2015, pp. 275-280.
DOI: 10.1016/j.infrared.2015.10.001

[40] G. Goett, R. Kozakov, D. Uhrlandt, H. Schoepp, A. Sperl, Emissivity and temperature determination on steel above the melting point, Weld World, vol. 57, 2013, p. 595–602.
DOI: 10.1007/s40194-013-0054-2

[41] G. Lee, S. Jeon, N. Yoo, C. Park, S. Park, Y. Su, S. Lee, Normal and directional spectral emittance measurement of semi transparent materials using two-substrate method: alumina, Int. Journal of Thermophysics, vol. 32, 2011, p. 1234–1246.
DOI: 10.1007/s10765-011-0986-y

[42] A. Adibekyan, High-accuracy Spectral Emissivity Measurement for Industrial and Remote Sensing Applications, 2018. Online [Accessed 21 May 2024] .
https://elekpub.bib.uni-wuppertal.de/urn/urn:nbn:de:hbz:468-20160421-144304-2

[43] L. M. Hanssen, S. Kaplan, Infrared diffuse reflectance instrumentation and standards at NIST, Analytica Chimica Acta, vol. 380, 1998, pp. 289-302.
DOI: 10.1016/S0003-2670(98)00669-2

[44] J. Hwang, H. Cho, D.-J. Shin, K. L. Jeong, Correction of port reflection effect for integrating sphere-based reflection measurements, Metrologia, vol. 50, 2013, p. 472–481.
DOI: 10.1088/0026-1394/50/5/472

[45] L. Hanssen, S. Mekhontsev, V. Khromchenko, (2004), Infrared Spectral Emissivity Characterization Facility at NIST, Thermosense|26|SPIE. Online [Accessed 21 May 2024] https://tsapps.nist.gov/publication/get_pdf.cfm?pub_id=841793

[46] L. M. Hanssen, C. P. Cagran, A. V. Prokhorov, Use of a High-Temperature Integrating Sphere Reflectometer for Surface Temperature Measurements, Int. Journal of Thermophysics, vol. 28, n. 2, 2007, pp. 566-580.
DOI: 10.1007/s10765-007-0180-4

[47] C. P. Cagran, L. M. Hanssen, Mart Noorma, A. V. Gura, Temperature-Resolved Infrared Spectral Emissivity of SiC and Pt–10Rh for Temperatures up to 900°C, Int. Journal of Thermophysics, vol. 28, n. 2, 2007, pp. 581-597.
DOI: 10.1007/s10765-007-0183-1

[48] D. Shi, Y. Liu, J. Sun, Z. Zhu, H. Liu, A new experimental apparatus for measurement of spectral emissivity of opaque materials using a reflector as the dummy light source, Int. Journal of Heat and Mass Transfer, vol. 55, 2012, pp. 3344-3348.
DOI: 10.1016/j.ijheatmasstransfer.2012.02.055

[49] Y. F. Zhang, J. M. Dai, Z. W. Wang, W. D. Pan, L. Zhang, A Spectral Emissivity Measurement Facility for Solar Absorbing

Coatings, Int J Thermophys, vol. 34, 2013, p. 916–925.
DOI: 10.1007/s10765-012-1171-7
[50] P. Giraud, J. Braillon, C. Delord, O. Raccurt, Development of optical tools for the characterization of selective solar absorber at elevated temperature, AIP Conf. Proc., vol. 1734, 2016, p. 130008.
DOI: 10.1063/1.4949218
[51] L. M. Hanssen, K. A. Snail, Integrating Spheres for Mid- and Near-infrared Reflection Spectroscopy, Handbook of Vibrational Spectroscopy, 2002, pp. 1-18.
DOI: 10.1002/0470027320.s2405
[52] L. M. Hanssen, S. N. Mekhontsev, J. Zeng, Evaluation of Blackbody Cavity Emissivity in the Infrared Using Total Integrated Scatter Measurements, Int. Journal of Thermophysics, vol. 29, 2008, p. 352–369.
DOI: 10.1007/s10765-007-0314-8
[53] A. Adibekyan, E. Kononogova, C. Monte, J. Hollandt, Review of PTB Measurements on Emissivity, Reflectivity and Transmissivity of Semitransparent Fiber-Reinforced Plastic Composites, Int. Journal of Thermophysics, vol. 40, n. 4, 2019, no. 36.
DOI: 10.1007/s10765-019-2498-0
[54] F. A. Yitagesu, F. v. d. Meer, H. v. d. Werff, C. Hecker, Spectral characteristics of clay minerals in the 2.5–14 µm wavelength region, Applied Clay Science„ vol. 53, 2011, pp. 581-591.
DOI: 10.1016/j.clay.2011.05.007
[55] J. Hameury, B. Hay, J. R. Filtz, Measurement of Infrared Spectral DirectionalHemispherical Reflectance and Emissivity atn BNM-LNE1, Int. Journal of Thermophysics, vol. 26, n. 6, 2005, pp. 1973-1983.
DOI: 10.1007/s10765-005-8609-0
[56] S. Moghaddam, J. Lawler, J. Currano, J. Kim, Novel Method for Measurement of Total Hemispherical Emissivity, Journal of thermophysics and heat transfer, vol. 21, n. 1, 2007, pp. 128-133.
DOI: 10.2514/1.26181
[57] K. Fukuzawa, A. O. &. Y. Nagasaka, Total Hemispherical Emittance of Polyimide Films for Space Use in the Temperature Range from 173 to 700 K, Int. Journal of Thermophysics, vol. 23, n. 1, 2002, pp. 319-331.
DOI: 10.1023/A:1013933917245
[58] M. Misale, G. Tanda, Measurement of total hemispherical emittance of solids using a steady-state calorimetric method, Proc. of the 6th Int. Symposium on Heat Transfer (ISHT-6), Beijing, China, 15-19 June 2004, pp.711-715.
[59] T. Fu, P. Tan, C. Pang, A steady-state measurement system for total hemispherical emissivity, Meas. Sci. Technol., vol. 23, 2012, p. 025006.
DOI: 10.1088/0957-0233/23/2/025006
[60] T. Fu, P. Tan, M. Duan, Simultaneous measurements of high-temperature total hemispherical emissivity and thermal conductivity using a steady-state calorimetric technique, Measurement Science and Technology, vol. 26, 2015, p. 015003.
DOI: 10.1088/0957-0233/26/1/015003
[61] A. Otsuka, K. Hosono, R. Tanaka, K. Kitagawa, N. Arai, A survey of hemispherical total emissivity of the refractory metals in practical use, Energy, vol. 30, 2005, p. 535–543.
DOI: 10.1016/j.energy.2004.04.019
[62] T. Matsumoto, A. Cezairliyan, A combined transient and brief steady-state technique for measuring hemispherical total emissivity of electrical conductors at high temperatures: Application to tantalum, Int. Journal of Thermophysics, vol. 28, n. 6, 1997, pp. 1539-1556.
DOI: 10.1007/BF02575350
[63] T. Matsumoto, A. Ono, A measurement technique for hemispherical total emissivity using feedback-controlled pulse current heating, High Temperatures High Pressure, vol. 32, n. 1, 2000, pp. 67-72.
DOI: 10.1068/htwu317
[64] H. Watanabe, T. Matsumoto, New analysis for determination of hemispherical total emissivity by feedback-controlled pulse-heating technique, Review of scientific instruments, vol. 76, 2005, p. 043904.
DOI: 10.1063/1.1884045
[65] J. Hameury, B. Hay, J. R. Filtz, Measurement of Total Hemispherical Emissivity Using a Calorimetric Technique, Int J Thermophys, vol. 28, 2007, p. 1607–1620.
DOI: 10.1007/s10765-007-0213-z
[66] J.-P. Monchau, J. Hameury, P. Ausset, B. Hay, L. Ibos, Y. Candau, Comparative study of radiometric and calorimetric methods for total hemispherical emissivity measurements, Heat Mass Transfer, vol. 54, 2018, p. 1415–1425.
DOI: 10.1007/s00231-017-2238-6
[67] Jean-Pierre Monchau, Hameury, J., Ausset, P., Hay, B., Laurent Ibos and Yves Candau (2017). Comparative study of radiometric and calorimetric methods for total hemispherical emissivity measurements. Heat and Mass Transfer, 54(5), pp.1415–1425.
DOI: 10.1007/s00231-017-2238-6
[68] T. Effertz, J. Pernpeintner, B. Schiricke, Steady state calorimetric measurement of total hemispherical emittance of cylindrical absorber samples at operating temperature, AIP Conf. Proc., vol. 1850, 2017, pp. 020003-1–020003-8.
DOI: 10.1063/1.4984327
[69] T. Fu, P. Tan, Transient Calorimetric Measurement Method forTotal Hemispherical Emissivity, Journal of Heat Transfer, vol. 134, , 2012 p. 11601.
DOI: 10.1115/1.4006896
[70] G. Tanda, M. Misale, Measurement of Total Hemispherical Emittance and Specific Heat of Aluminum and Inconel 718 by a Calorimetric Technique, Transactions of the ASME, vol. 128, 2006, pp. 302-306.
DOI: 10.1115/1.2150840
[71] T. Fu, P. Tan, M. Zhong, Experimental research on the influence of surface conditions on the total hemispherical emissivity of iron-based alloys, Experimental Thermal and Fluid Science, vol. 40, 2012, pp. 159-167.
DOI: 10.1016/j.expthermflusci.2012.03.001
[72] B. Yang, S. Zhang, W. Zhai, M. Li, L. Yang, l. Xiong, Steady-state Calorimetry Measurement Method for Total Hemispherical Emissivity of Thermal Insulating Coating, IOP Conf. Ser.: Earth Environ. Sci., vol. 170 , p. 042105, 2018.
DOI: 10.1088/1755-1315/170/4/042105
[73] J. K. C.M. Schneider, Chapter 9 - Magnetism at Surfaces and in Ultrathin Films, in Handbook of Surface Science, vol. 2, K. Horn, M. Scheffler, 2000, pp. 511-668.
DOI: 10.1016/B978-012513910-6/50028-1
[74] G. Venugopal, M. Deiveegan, C. Balaji, S. P. Venkateshan, Simultaneous retrieval of total hemispherical emissivity and specific heat from transient multimode heat transfer experiments, Journal of heat transfer, vol. 130, n. 6, 2008, p. 061601.
DOI: 10.1115/1.2891221
[75] Y. M. Guo, S. J. Pang, Z. J. Luo, Y. Shuai, H. P. Tan, H. Qi, Measurement of Directional Spectral Emissivity at High Temperatures, Int. Journal of Thermophysics, vol. 40, 2019, pp. 1-12.
DOI: 10.1007/s10765-018-2472-2
[76] P. L. Wang, S. Basu, M. Z. Zhang, Direct measurement of thermal emission from a Fabry–Perot cavity resonator, Journal of heat transfer, vol. 134, 2012, pp. 1-9.
DOI: 10.1115/1.4006088
[77] Y. C. Niu, H. Qi, T. Y. Ren, M. L. Ruan, Apparent directional spectral emissivity determination of semitransparent materials, Chinese Physics B, vol. 25, n. 4, 2016, pp. 1-13.
DOI: 10.1088/1674-1056/25/4/047801
[78] K. Yu, R. Tong, K. Zhang, Y. Liu, Y. Liu, An Apparatus for the Directional Spectral Emissivity Measurement in the Near Infrared Band, Int. Journal of Thermophysics, 2021, pp. 42-80.
DOI: 10.1007/s10765-021-02813-0
[79] Y. Sun, C. Lou, H. Zhou, A simple judgment method of gray property of flames based on spectral analysis and the two-color method for measurements of temperatures and emissivity, Proc.

of the Combustion Institute, vol. 33, 2011, pp. 735-741. DOI: 10.1016/j.proci.2010.07.042
[80] W. Yan, A. Panahi, Y. A. Levendis, Spectral emissivity and temperature of heated surfaces based on spectrometry and digital thermal imaging – Validation with thermocouple temperature measurements, Experimental Thermal and Fluid Science, vol. 112, 2020. DOI: 10.1016/j.expthermflusci.2019.110017
[81] S. Zheng, Y. Yang, X. Li, H. Liu, W. Yan, R. Sui, Q. Lu, Temperature and emissivity measurements from combustion of pine wood, rice husk and fire wood using flame emission spectrum, Fuel Processing Technology, vol. 204, 2020. DOI: 10.1016/j.fuproc.2020.106423
[82] R. M. Sova, M. J. Linevsky, M. E. Thomas, F. F. Mark, High-temperature infrared properties of sapphire, AlON, fusedsilica, yttria, and spinel, Infrared Physics & Technology, vol. 39, p. 251–261, 1998. DOI: 10.1016/S1350-4495(98)00011-5
[83] O. Rozenbaum, D. S. Meneses, Y. Auger, S. Chermanne, P. Echegut, A spectroscopic method to measure the spectral emissivity of semi-transparent materials up to high temperature, American Institute of Physics, vol. 70, n. 10, 1999, pp. 4020-4025. DOI: 10.1063/1.1150028
[84] M. J. Ballico, T. P. Jones, Novel Experimental Technique for Measuring High-Temperature Spectral Emissivities, Applied Spectroscopy, vol. 49, pp. 335-340, 1995. DOI: 10.1366/0003702953963
[85] V. S. Dozhdikov, V. A. Petrov, New experimental facility for measurement of total and spectral emissivities of various thermal protection materials and coatings at high temperatures, High Temperatures. High Pressures, vol. 27, n. 4, 1996, pp. 411-422. DOI: 10.1068/htrt90
[86] C. Monte, B. Gutschwager, S. P. Morozova, J. Hollandt, Radiation Thermometry and Emissivity Measurements Under Vacuum at the PTB, Int J Thermophys, vol. 30, 2009, p. 203–219. DOI: 10.1007/s10765-008-0442-9
[87] A. Adibekyan, C. Monte, M. Kehrt, B. Gutschwager, J. Hollandt, Emissivity Measurement Under Vacuum from 4 µm to 100 µm and from −40 °C to 450 °C at PTB, Int J Thermophys., vol. 36, 2015, p. 283–289. DOI: 10.1007/s10765-014-1745-7
[88] K. Zhang, Y. Liu, Modified two-temperature calibration method for emissivity measurements at high temperatures, Applied Thermal Engineering, vol. 168, 2020. DOI: 10.1016/j.applthermaleng.2019.114854
[89] L. d. Campo, B. R. Pérez-Sáez, L. González-Fernández, X. Esquisabel, I. Fernández, P. González-Martín, M. J. Tello, Emissivity measurements on aeronautical alloys, Journal of alloys and compounds, vol. 489, 2010, p. 482–487. DOI: 10.1016/j.jallcom.2009.09.091
[90] I. G. d. Arrieta, T. Echániz, R. Fuente, E. Rubin, R. Chen, J. Igartua, M. Tello, G. López, Infrared emissivity of copper-alloyed spinel black coatings for concentrated solar power systems, Solar Energy Materials and Solar Cells, vol. 200, 2019, p. 10996. DOI: 10.1016/j.solmat.2019.109961
[91] L. Mercatelli, M. Meucci, E. S. , Facility for assessing spectral normal emittance of solid materials at high temperature, Applied Optics, vol. 54, 2015, pp. 8700-8705. DOI: 10.1364/AO.54.008700
[92] E. Lindermeir, V. Tank, P. Haschberger, Contactless measurement of the spectral emissivity and temperature of surfaces with a Fourier transform infrared spectrometer, Thermosense XIV: An Intl Conf on Thermal Sensing and Imaging Diagnostic Applications, vol. 1682, pp. 354-364, 1992. DOI: 10.1117/12.58553
[93] J. Dai, X. Wang, G. Yuan, Fourier transform spectrometer for spectral emissivity measurement in the temperature range between 60 and 1500°C, in 7th Int. Symposium on Measurement Technology and Intelligent Instruments, 2005. DOI: 10.1088/1742-6596/13/1/015
[94] C. D. Wen, I. Mudawar, Emissivity characteristics of polished aluminum alloy surfaces and assessment of multispectral radiation thermometry (MRT) emissivity models, Int. Journal of Heat and Mass Transfer, vol. 48, p. 1316–1329, 2004. DOI: 10.1016/j.ijheatmasstransfer.2004.10.003
[95] T. Pierre, J.-C. Krapez, H. R. Orlande, C. Rodiet, D. Le Maux, M. Courtois, P. Le Masson, B. Lamien, Simultaneous estimation of temperature and emissivity of metals around their melting points by deterministic and Bayesian techniques, Int. Journal of Heat and Mass Transfer, 2022, p. 122077. DOI: 10.1016/j.ijheatmasstransfer.2021.122077
[96] D. A. Houtz, D. Gu, A Measurement Technique for Infrared Emissivity of Epoxy-Based Microwave Absorbing Materials, IEEE Geoscience and Remote Sensing Letters , vol. 15, 2018, pp. 1-10. DOI: 10.1109/LGRS.2017.2772783
[97] M. Ball, H. Pinkerton, Factors affecting the accuracy of thermal imaging cameras in volcanology, Journal of Geophysical Research, vol. 111, 2006, p. B11203. DOI: 10.1029/2005JB003829
[98] O. Riou, P.-O. Logerais, J.-F. Durastanti, Quantitative study of the temperature dependence of normal LWIR apparent emissivity, Infrared Physics and Technology, vol. 60, 2013, pp. 244-250. DOI: 10.1016/j.infrared.2013.05.012
[99] D. Shi, F. Zou, S. Wang, Z. Zhu, J. Sun, B. Wang, Spectral emissivity modeling of steel 201 during the growth of oxidation film over the temperature range from 800 to 1100K in air, Infrared Physics & Technology, vol. 67, 2014, pp. 42-48. DOI: 10.1016/j.infrared.2014.07.004
[100] A. Jeromen, I. Grabec, E. Govekar, Laser pulse transient method for measuring the normal spectral emissivity of samples with arbitrary surface quality, Appl Phys A, vol. 92, p. 945–949, 2008. DOI: 10.1007/s00339-008-4601-4
[101] E. Planas-Cuchi, J. M. Chatris, C. Lopez, J. Arnaldos, Determination of Flame Emissivity in Hydrocarbon Pool Fires Using Infrared Thermography, Fire Technology, 39, vol. 39, 2003, p. 261–273. DOI: 10.1023/A:1024193515227
[102] E. Pastor, A. Rigueiro, L. Zárate, A. Giménez, J. Arnaldos, E. Planas, Experimental methodology for characterizing flame emissivity of small scale forest fires using infrared thermography techniques, Forest Fire Research & Wildland Fire Safety, pp. 1-11, 2002, ISBN 90-77017-72-0.
[103] J. Yang, M. S. Wong, M. Menenti, J. Nichol, J. Voogt, E. S. Krayenhoff, P. Chan, Development of an improved urban emissivity model based on sky view factor for retrieving effective emissivity and surface temperature over urban areas, ISPRS Journal of Photogrammetry and Remote Sensing, 2016, pp. 30-40. DOI: 10.1016/j.isprsjprs.2016.09.007
[104] F. Albouchi, F. Mzali, F. Rigollet, S. B. Nasrallah, Effective Emissivity Measurements of Powders and Their Mixtures, Journal of Porous Media, vol. 10, 2007, n. 2. DOI: 10.1615/JPorMedia.v10.i2.60
[105] E. Barreira, E. Bauer, N. Mustelier, V. Freitas, Measurement of materials emissivity - Influence of the procedure, Proc. of the 13th Int. Workshop on Advanced Infrared Technology & Applications, Pisa, pp. 242-245, 2015.
[106] K. Schurer, A Method for Measuring Infrared Emissivities of Near-Black Surfaces at Ambient Temperatures, Int. Conf. on Infrared Physics (CIRP), 1976, pp. 157-163.
[107] T. Inagaki, Y. Okamoto, Surface temperature measurement near ambient conditions using infrared radiometers with different detection wavelength bands by applying a grey-body approximation: estimation of radiative properties for non-metal surfaces, NDT & E International, vol. 29, n. 6, 1996, pp. 363-369. DOI: 10.1016/S0963-8695(96)00039-4
[108] K. Chrzanowski, Problem of Determination of Effective Emissivity of Some Materials In MIR Range, Infrared Phys. Technol., vol. 36, n. 3, 1995, pp. 679-684. DOI: 10.1016/1350-4495(94)00107-V

[109] D. Especel, S. Mattei, Total emissivity measurements without use of an absolute reference, Infrared Physics & Technology, vol. 37, 1996, pp. 777-784.
DOI: 10.1016/S1350-4495(96)00017-5
[110] C. McDaid, Y. Zhang, Wall temperature measurements using a thermal imaging camera, Meas. Sci. Technol., vol. 22, 2011, p. 125503.
[111] E. Pastor, A. Rigueiro, L. Zárate, A. Giménez, J. Arnaldos, E. Planas, Experimental methodology for characterizing flame emissivity of small scale forest fires using infrared thermography techniques, IV Int. Conf. on Forest Fire Research , pp. 1-11, 2002.
[112] P. Hagqvist, F. Sikström, A.-K. Christiansson, Emissivity estimation for high temperature radiation pyrometry on Ti–6Al–4V, Measurement, vol. 46, 2013, p. 871–880.
DOI: 10.1016/j.measurement.2012.10.019
[113] C. Purpura, E. Trifoni, M. Musto, G. Rotondo, R. Ragione, Methodology for spectral emissivity measurement by means of single color pyrometer, Measurement, 2016.
DOI: 10.1016/j.measurement.2016.01.018
[114] G. Neuer, G. Jaroma-Weiland, Spectral and Total Emissivity of High-Temperature Materials, Int. Journal of' Thermophysic, vol. 19, n. 3, 1998, pp. 917-929.
DOI: 10.1023/A:1022607426413
[115] R. Brandt, C. Bird, G. Neuer, Emissivity reference paints for high temperature applications, Measurement, vol. 41, 2008, p. 731–736.
DOI: 10.1016/j.measurement.2007.10.007
[116] C.-G. Ren, Y.-L. Lo, H.-C. Tran, M.-H. Lee, Emissivity calibration method for pyrometer measurement of melting pool temperature in selective laser melting of stainless steel 316, The Int. Journal of Advanced Manufacturing Techno, vol. 105, 2019, p. 637–649.
DOI: 10.1007/s00170-019-04193-0
[117] B. Müller, U. Renz, Development of a fast fiber-optic two-color pyrometer for the temperature measurement of surfaces with varying emissivities, Review of scientific instruments, vol. 72, n. 8, 2001, pp. 366-3374.
DOI: 10.1063/1.1384448
[118] J. Thevenet, M. Siroux, B. Desmet, Measurements of brake disc surface temperature and emissivity by two-color pyrometry, Applied Thermal Engineering, vol. 30, 2010, p. 753–759.
DOI: 10.1016/j.applthermaleng.2009.12.005
[119] S. Krenek, K. Anhalt, A. Lindemann, C. Monte, J. Hollandt, J. Hartmann, A Study on the Feasibility of Measuring the Emissivity with the Laser-Flash Method, Int. Journal of Thermophysics, vol. 31, 2010, p. 998–1010.
DOI: 10.1007/s10765-010-0767-z
[120] C. Zhu, M. J. Hobbs, J. R. Willmott, An accurate instrument for emissivity measurements by direct and indirect methods, Measurement Science and Technology, vol. 31, 2020, pp. 1-13.
DOI: 10.1088/1361-6501/ab5e9b
[121] J. N. G. S. E. &. T. R. Fischer, Metrological characterisation of a new transfer-standard radiation thermometer, in Proc. TEMPMEKO2001, Int. Symp. on Temperature and Thermal Measurements in Industry and Science, Berlin, Germany, 2001.
DOI: 10.5194/jsss-9-425-2020
[122] C. McDaid, Y. Zhang, Wall temperature measurements using a thermal imaging camera with temperature-dependent emissivity corrections, Measurement Science and Technology, 2011, p. 125503 (8pp).
DOI: 10.1088/0957-0233/22/12/125503
[123] JCGM, Evaluation of measurement data-Guide to the expression of uncertainty in measurement Évaluation des données de mesure-Guide pour l'expression de l'incertitude de mesure, 2008.
[124] I. VIM, Int. vocabulary of basic and general terms in metrology (VIM), Int. Organization, 2004, pp. 09-14.